NANO LETTERS

2008
Vol. 8, No. 1
265−270

Mesoporous Co_3O_4 Nanowire Arrays for Lithium Ion Batteries with High Capacity and Rate Capability

Yanguang Li, Bing Tan, and Yiying Wu*

Department of Chemistry, The Ohio State University, 100 West 18th Avenue, Columbus, Ohio 43210

Received October 8, 2007; Revised Manuscript Received November 28, 2007

ABSTRACT

We report the high capacity and rate capability of mesoporous Co_3O_4 nanowire (NW) arrays as anodes in Li ion batteries. At a current of 1C, the NW arrays maintain a capacity of 700 mAh/g after 20 discharge/charge cycles. When the current is increased to 50C, 50% of the capacity can be retained. With their ease of large area synthesis and superior electrochemical properties, these Co_3O_4 NW arrays will be interesting for practical Li ion batteries.

Self-supported nanowire (NW) arrays growing directly on a current-collecting substrate represent an attractive architecture for Li ion battery electrode.[1−8] The open space between neighboring NWs allows for easy diffusion of electrolyte into the inner region of the electrode, resulting in reduced internal resistance and improved high-power performance. Each NW has its own contact with the substrate at the bottom. This can ensure every NW participates in the electrochemical reaction. Using NW arrays also saves the tedious process of mixing active material with ancillary materials such as carbon black and polymer. Moreover, NWs share the same advantages as other nanostructured electrodes with high electrode−electrolyte contact area, fast Li^+ ion diffusion, and good strain accommodation.[9,10]

Previously reported research on NW-array electrode has utilized the template-synthesis method. Martin and co-workers have pioneered this method using porous membranes as the template and synthesized NW arrays made of carbon, TiS_2, $LiMn_2O_4$, and $LiFePO_4$. The electrode reactions involve the insertion (or extraction) of Li^+ ions with the charge compensated by the addition (or removal) of electrons. More recently, Taberna et al. extended the idea to Fe_3O_4, operated by the conversion reaction mechanism,[11] in which the metal oxide (M_xO_y) reacts with Li^+ ions and forms metal nano-domains (M^0) dispersed in Li_2O matrix. High capacity and rate-capability have been demonstrated using these NW arrays as electrodes. Despite these progresses, template synthesis is difficult to produce large-area NW arrays limited by the membrane template. Moreover, for electrode materials with poor electric conductivity such as TiS_2 and Fe_3O_4, the previously reported approach was to attach them to metal NWs and form core−shell structures.[1,8] This will further increase the complexity of material processing and reduce the specific capacity due to the additional weight of the metal NWs.

In this study, we utilized a mild template-free method for large-area growth of self-supported Co_3O_4 NW arrays. Co_3O_4 has been demonstrated to be a promising anode material.[11−18] The NW arrays were synthesized by an ammonia-evaporation-induced method modified from our previous report.[19] Specifically, 10 mmol $Co(NO_3)_2$ and 5 mmol NH_4NO_3 were dissolved in 15 mL of 30 wt % ammonia solution and 35 mL of H_2O. The homogeneous solution was magnetically stirred for half an hour in air during which the original pink color gradually turned into black. This color change indicates the oxidation from Co(II) to Co(III) in solution by the uptake of oxygen. Then the solution was transferred to a covered petri dish and heated in an oven at 90 °C for 2 h. After that, a clean substrate such as a Ti foil fixed with a Teflon clamp was introduced into the reaction solution. The solution was heated for an additional 12 h at the same temperature for the NW growth. Before battery testing, the NW arrays were treated at 250 °C for 2 h to remove the trapped and adsorbed water.

The Co_3O_4 NW arrays have been successfully grown on various substrates such as Si wafer, glass slide, Cu or Ti foil, and polystyrene substrate. Here, we have chosen Ti foil as the conducting substrate because Ti is very resistive to the alkaline ammonia solution and oxidation. Furthermore, Ti does not alloy with metallic lithium at low voltage and therefore is a good current collector material for battery testing.[20] Figure 1a shows the photograph of a Ti foil coated

* To whom correspondence should be addressed. E-mail: wu@chemistry.ohio-state.edu.

10.1021/nl0725906 CCC: $40.75
Published on Web 12/12/2007

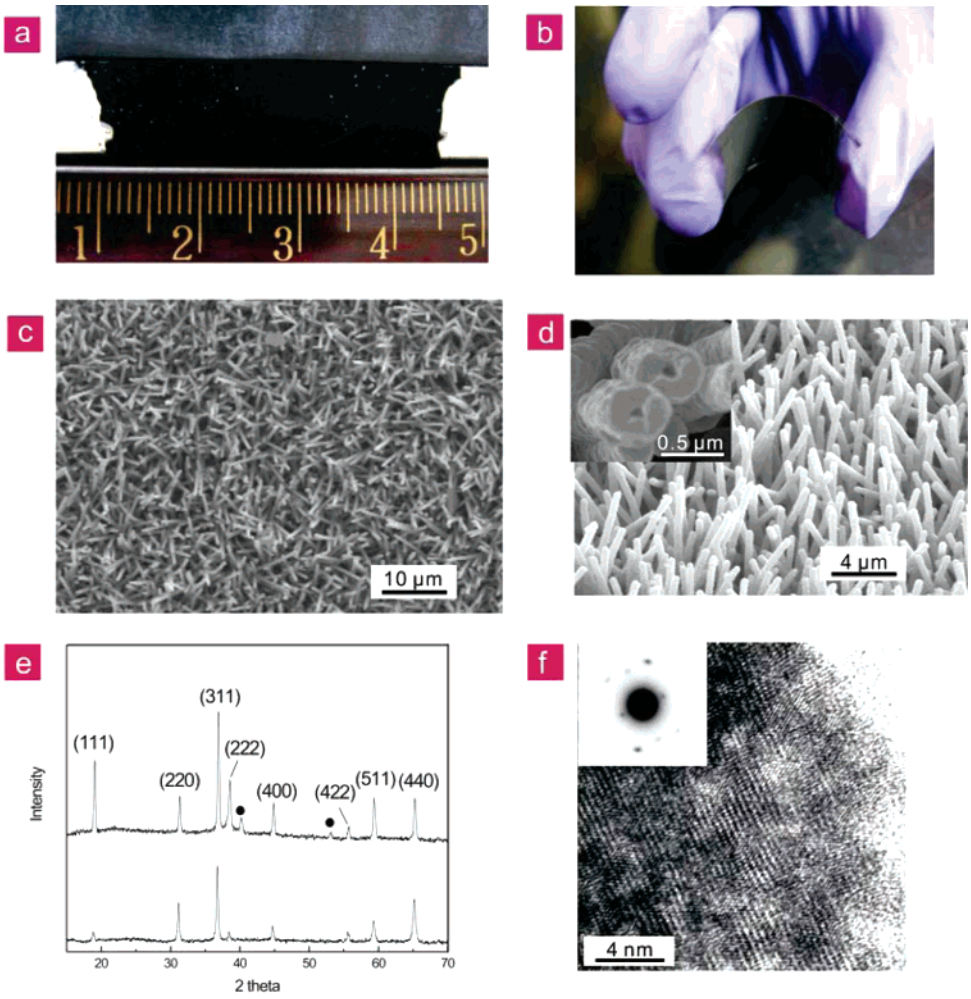

Figure 1. Morphology and structural characterizations of the Co_3O_4 NW arrays. (a,b) Photographs of the Co_3O_4 NW arrays on Ti foil (a) and conductive plastic substrate (b); (c,d) SEM images of Co_3O_4 NW arrays growing on Ti foil viewed from the top (c) and when tilted by 40° (d). The inset of d shows the open tips of the NWs. (e) XRD patterns of standard Co_3O_4 powder (bottom) and the as-prepared Co_3O_4 nanowire arrays growing on Ti foil (top). The diffraction peaks can be indexed as spinel Co_3O_4 exclusively, and (●) denotes diffraction peaks from the Ti substrate. (f) HRTEM image of a Co_3O_4 NW and the corresponding SAED pattern (inset).

with a layer of black NWs. We would also like to point out that the NW arrays can grow on conductive plastic substrates. The mild growth process does not damage the conductivity of the substrate. As shown in Figure 1b, the substrate with the NW coating can be easily bent without damage to the NWs, making them interesting for flexible batteries.[15,17]

The structural characterization of the as-prepared Co_3O_4 NW arrays on Ti foil is shown in Figure 1c−f. Each NW is about 500 nm in diameter and about 15 μm in length. They grow almost vertically from the substrate. The X-ray diffraction (XRD) pattern of the NW arrays shows unusually strong (111) diffraction peak in comparison with that of the powders (Figure 1e top versus bottom), indicating the [111] growth direction of the NWs. The NWs are tubular with open tips (Figure 1d, inset). As shown in our previous report,[19] the Co_3O_4 NWs are single-crystalline and mesoporous, resulting from the topotactic transformation from $Co(OH)_2$ to Co_3O_4 during the growth process. The average pore size is 3.3 nm. The single-crystalline nature of the NWs is shown in the high-resolution transmission electron microscopy (HRTEM) and the selected area electron diffraction (SAED) pattern (Figure 1f and inset). In average, 2−3 mg NWs are grown on 1 cm^2 Ti foil.

Figure 2a is the voltage-capacity profile of the first two discharge/charge cycles of our NW array sample at a current of 1C (1C is defined as one lithium per formula in an hour, that is 111 mA/g for Co_3O_4). During the first discharge, it exhibits a distinct plateau at 1.0 V versus Li^+/Li^0 for 7.6 Li^+ uptake, followed by a gradual slope equivalent to another 1.9 Li^+ uptake. The total capacity for the first discharge reaches 1124 mAh/g. Subsequent charge curve shows a large voltage hysteresis, which is a signature of conversion reaction mechanism.[8,11] Only 859 mAh/g was recovered after the first full charge. To find out the origin of this capacity loss, we have used XRD and TEM to investigate the compositional and structural changes at different stages of the electrochemical reaction. When the cell was completely discharged, the diffraction peaks of Co_3O_4 disappeared in the XRD pattern. A peak at 32.6° and a broad weak peak at 44.2° appeared instead, assigned to Li_2O (111) and Co (111), respectively, (Figure 2b, middle). This is consistent with the conversion reaction mechanism in which Co_3O_4 is reduced, forming

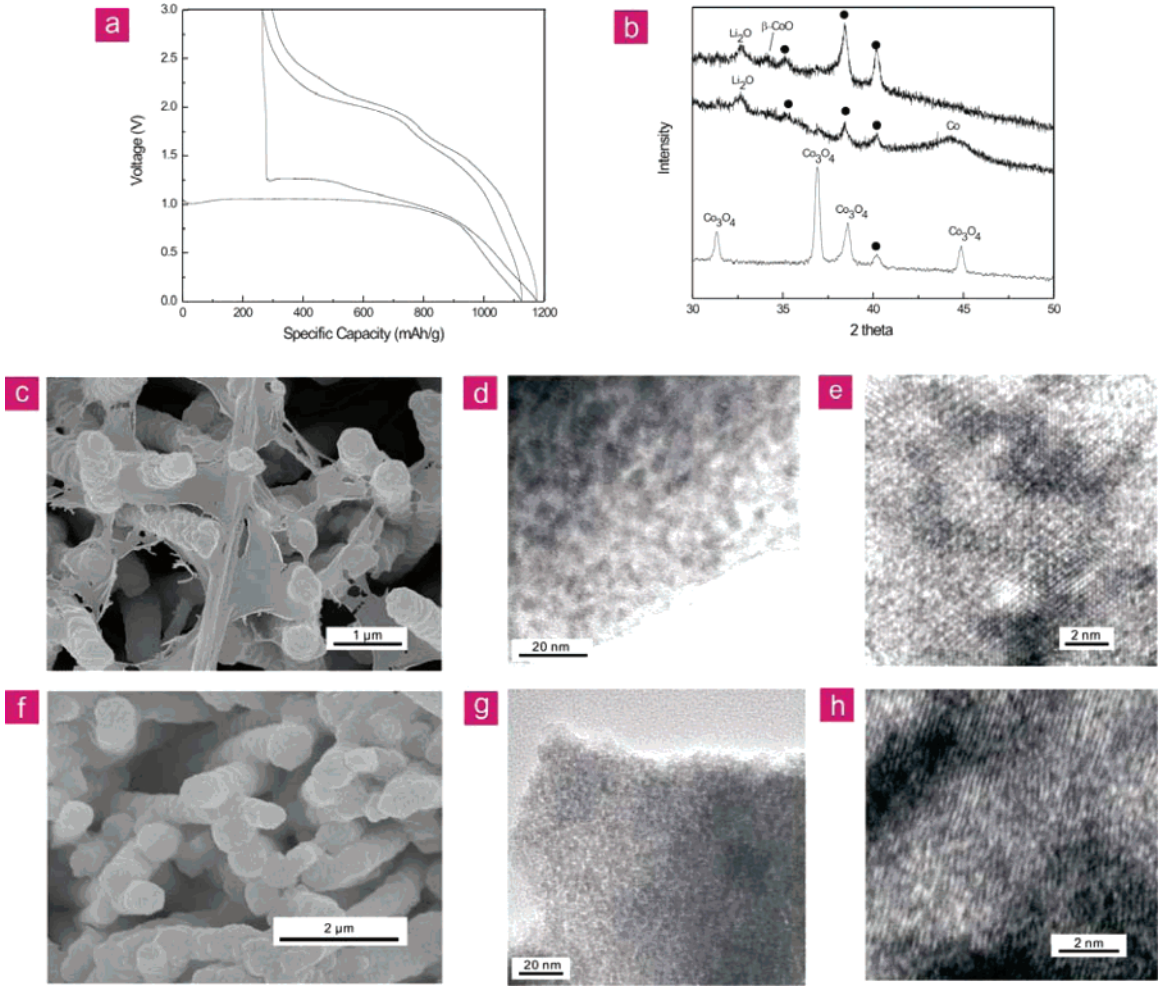

Figure 2. (a) The charge/discharge curve of Co_3O_4 NW arrays for the first 2 cycles at 1C. (b) XRD patterns of as-prepared sample (bottom), discharged sample (middle), and recharged sample (top). (●) denotes diffraction peaks from the Ti substrate. (c) SEM image of discharged NW arrays with polymeric film on the top. (d,e) TEM images of discharged sample. The lattice fringes in (e) match the structure of metallic Co. (f) SEM image of recharged NW arrays. (g,h) TEM images of recharged sample. The lattice fringes in (h) match β-CoO.

metallic Co nanodomains embedded in the Li_2O matrix.[11] The scanning electron microscopy (SEM) image of the discharged sample shows that the NW morphology is preserved except that the top of the arrays are coated with polymeric films (Figure 2c). The organic nature of this film was verified by the Fourier transform IR (FTIR) transmission spectrum (see Supporting Information, Figure SI-1). Laruelle et al. proposed that the polymeric films result from the catalytically enhanced electrolyte reduction at low potential.[21] TEM characterization reveals the formation of nanosized metallic Co grains (dark regions in Figure 2d, domain size ~3 nm). The lattice fringes in HRTEM match with the structure of cobalt (Figure 2e). The small grain size explains the broad and weak Co peak observed in the XRD pattern.

When charging the cell back to 3.0 V, we observed that the broad and weak Co peak vanished in the XRD pattern, but no Co_3O_4 peaks reappeared. Instead, a weak peak at 34.2° appeared that can be assigned to β-CoO (111) planes. These results indicate that β-CoO is the recovered species after the first full electrochemical cycle. The loss of 2 Li per Co_3O_4 formula due to this $Co_3O_4 \rightarrow$ CoO transformation is the main cause of the large capacity loss during the first cycle. This is consistent with several previous reports on the electrochemical reactivity of Co_3O_4 powders.[13,17,22] Despite the compositional transformation, it is important to observe that the NW arrays maintained their structure integrity after charging the cell back as shown in the SEM image (Figure 2f). Our subsequent investigation has demonstrated that the NW arrays can survive tens of cycles with only slight deformation like bending due to the pressure applied by the counter electrode during testing (see Supporting Information, SI-2). Retaining the structure integrity is a key factor to ensure the cycleability of our material. It is also noteworthy that the polymeric films were dissolved upon being charged back. This reversible formation/dissolution process of the polymeric film is consistent with a previous report by Laruelle.[21] TEM analysis reveals that the NWs after the first cycle are nanotextured, and the lattice fringes match the structure of β-CoO. Through the above results, we can conclude that the NW arrays can maintain their structural integrity during the first electrochemical cycle with transformation of composition from the initial Co_3O_4 to Co and then to β-CoO.

After the first discharge/charge cycle, the subsequent cycles showed high reversibility. The NW arrays maintain a stable capacity at 700 mAh/g after 20 cycles (Figure 3a,

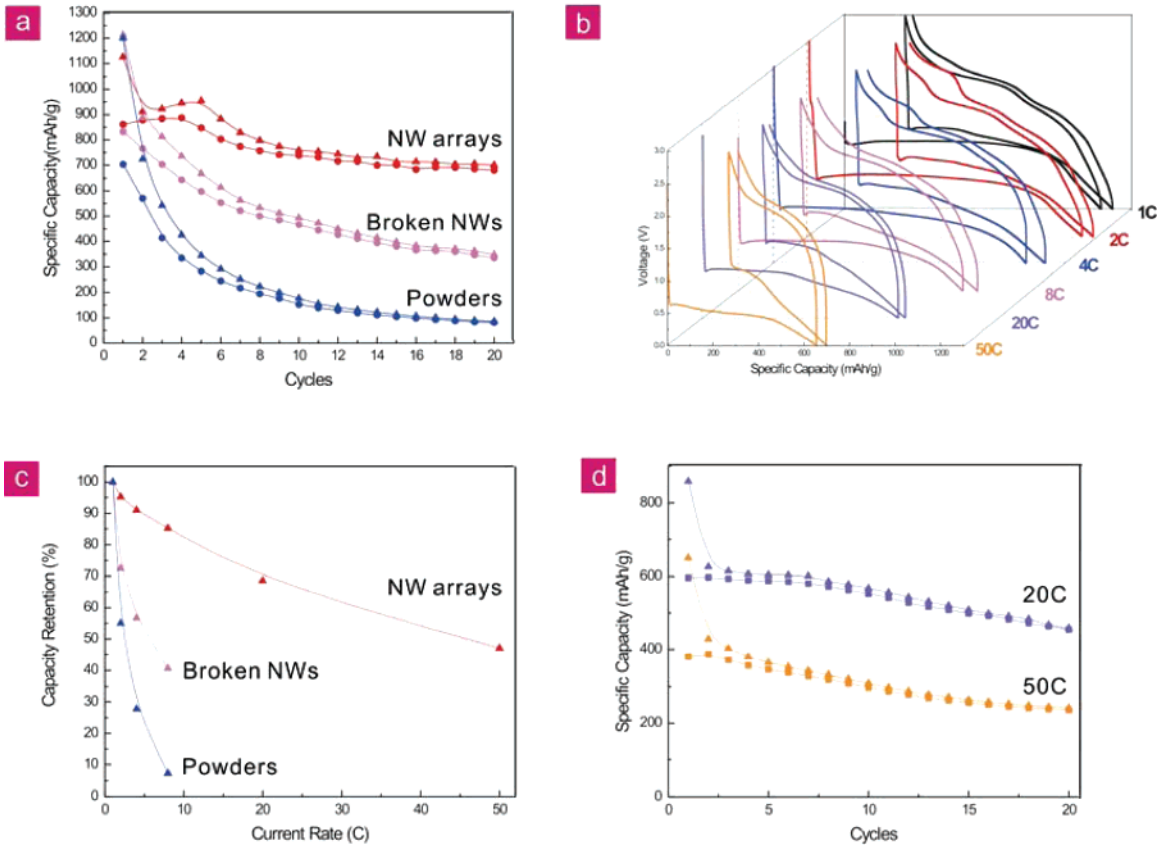

Figure 3. Measurements of capacity and rate capability. (a) Specific capacity of the Co_3O_4 NW arrays on Ti foil (red), non-self-supported NWs (magenta), and commercial powders (blue) as a function of the cycle number. For each set of data, the upper curve is for discharge and the lower curve is for charge. (b) Charge/discharge curves of the NW arrays at various current rates from 1 to 50C. (c) Capacity retention percentage of the NW arrays (red), broken NWs (magenta), and powders (blue) as a function of the current rate based on the discharge capacity during the second cycle. (d) Specific capacity of the NW arrays at 20C (violet) and 50C (orange) as a function of the cycle number.

top curve). For the purpose of comparison, we have prepared two other samples made of non-self-supported NWs and commercial powders, respectively, mixed with carbon black and polymer binder (see Supporting Information). Under the same condition, commercial powders give a poor capacity of 80 mAh/g and non-self-supported NWs only have a moderate 350 mAh/g after 20 cycles (Figure 3a, bottom and middle curves, respectively). Carbon is the anode material used in commercial Li ion batteries and can be considered as the benchmark anode material. The theoretical capacity is 372 mAh/g for graphite. Therefore, the Co_3O_4 NW array reported here shows a capacity close to twice of the graphite. In previous literature references, there are only a few papers about free-standing NW array anodes prepared by the cumbersome template-synthesis method, including the carbon nanotube membrane (490 mAh/g),[3] the SnO_2 NW arrays (~700 mAh/g),[5] and the Fe_3O_4/Cu composite NW arrays (~800 mAh/g).[8] In addition, there are papers about random nanowire/nanotube anodes, such as multiwall carbon nanotubes (320 mAh/g),[23] TiO_2 (305 mAh/g),[24] SnO_2 (~400 mAh/g),[25] Co_3O_4 (~500 mAh/g),[26] CuO (~500 mAh/g),[27] Fe_2O_3 (510 mAh/g),[28] and MoO_3 (150 mAh/g).[29] By comparison, it is easy to tell that our Co_3O_4 NW arrays show one of the best capacities among the reported NW anode materials.

We have also tested the performance of NW arrays at higher currents varied from 2 to 50C (Figure 3b), because the rate capability is an important parameter for many applications of batteries such as electric vehicles and portable power tools, which require fast discharge and/or charge rate. If we compare the discharge capacity of the second cycle at various currents, the NW arrays can retain 85% capacity at 8C, 69% at 20C, and 50% at 50C relative to the capacity at 1C (Figure 3c, top curve). In contrast, the capacity of non-self-supported NWs or powders decays much more sharply with the increase of current (Figure 3c, middle and bottom curves). For example, the powder sample has only 8% retention at 8C. Moreover, the NW arrays show good cycleability at high currents. Figure 3d shows the specific capacity of the first 20 cycles at 20 and 50C. After 20 cycles, the NW arrays can still maintain a capacity of 450 mAh/g at 20C and 240 mAh/g at 50C. The rate capability of our NW arrays surpasses most previously published results on Co_3O_4.[11,12,14,30,31] The only comparable report is from Nam et al. using Co_3O_4−Au hybrid NWs synthesized by the genetically engineered virus-templating method.[15]

We believe the high capacity and rate capability of the NW arrays come from the unique hierarchical architecture. First, the NW array configuration can ensure that every NW participates in the electrochemical reaction, because every

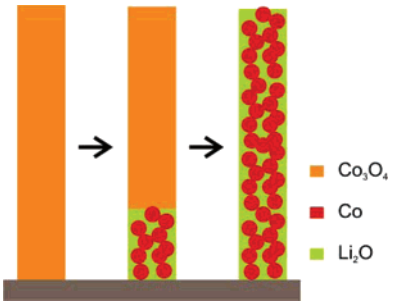

Figure 4. Schematic illustration of the electrochemical reduction of Co_3O_4 NW, starting from the NW root region and then gradually propagating through the NW. The formed Co nanodomains are interconnected.

nanowire is in electric contact with the Ti substrate and also interfaced with the electrolyte solution. Second, the open space between neighboring NWs allows for easy diffusion of the electrolyte. This feature is particularly helpful for high power applications when the battery is charged or discharged at high current. Third, the NWs in this study are mesoporous with an average pore size of 3.3 nm and a BET surface area of 73.5 m^2/g as shown in our previous investigation.[19] The porosity will enhance the electrolyte/Co_3O_4 contact area, shorten the Li^+ ion diffusion length in the NWs, and accommodate the strain induced by the volume change during the electrochemical reaction. As a result, our mesoporous NW arrays can achieve a good cycleability and high rate capability. In comparison, the conventional electrode preparation method requires a thorough mixing of active materials with ancillary materials, which is then pressed onto a conducting substrate to improve its mechanic strength and prevent it from peeling off the substrate. This process is tedious, and a complete homogeneous mixing is difficult to achieve due to the particle aggregation.[17] The process will also unavoidably cause some locally coalesced regions that are inaccessible to the electrolyte solution and lose the original nanosized feature of the active material.[8] The poorly controlled porous geometry in the conventional electrodes also limits the mass transport of the electrolyte solution into the deep region of the electrode.

To fully explain the superior performance of the NW arrays, we still need to address the question of how the electrons are conducted in the NWs. In the charged state, the NWs are made of Co_3O_4 or CoO. When completely discharged, they are reduced to Co nanograins embedded in Li_2O matrices. Co_3O_4, CoO, and Li_2O are all poor electron conductors. In previous reports on Co_3O_4,[11,14,15,17] carbon black was added to improve the electric conductivity. However, no carbon or other ancillary materials have been used in our investigation. To explain the electron-conducting mechanism of our NWs, we suggest the Co nanodomains are in contact with each other and form interconnected network. For each Co_3O_4 NW, the electrochemical reaction takes place first at the root region that is in direct contact with the Ti substrate and then gradually propagates through the whole NW (Figure 4). Such a mechanism can also explain the high performance of the dense Co_3O_4 and CuO thin film electrodes that had been directly coated on conducting substrates without ancillary materials.[13,32]

In summary, self-supported Co_3O_4 NW arrays growing on Ti foil have been tested as the anode for lithium ion batteries. A mild template-free method has been developed for large-area NW growth, and the resulting NW arrays can be directly used for batteries without adding any ancillary materials. The NW arrays have shown high capacity, good cycleability and high rate capability. We believe that their outstanding performance comes from the unique hierarchical architecture of the mesoporous NWs. With their ease of fabrication and good performance, these NW arrays will hold promise in practical Li ion batteries.

Acknowledgment. The project was sponsored by the start-up fund from The Ohio State University. We thank K. Wolken for assistance in microtomy.

Supporting Information Available: The details of NW synthesis, characterization and battery measurements, FTIR spectrum of the completely discharged sample, and SEM image of the NW array electrode after 20 cycles. This material is available free of charge via the Internet at http://pubs.acs.org.

References

(1) Che, G.; Jirage, K. B.; Fisher, E. R.; Martin, C. R. *J. Electrochem. Soc.* **1997**, *144*, 4296−4302.
(2) Nishizawa, M.; Mukai, K.; Kuwabata, S.; Martin, C. R.; Yoneyama, H. *J. Electrochem. Soc.* **1997**, *144*, 1923−1927.
(3) Che, G.; Lakshmi, B. B.; Fisher, E. R.; Martin, C. R. *Nature* **1998**, *393*, 346−349.
(4) Li, N.; Patrissi, C. J.; Che, G.; Martin, C. R. *J. Electrochem. Soc.* **2000**, *147*, 2044−2049.
(5) Li, N.; Martin, C. R. *J. Electrochem. Soc.* **2001**, *148*, A164−A170.
(6) Patrissi, C. J.; Martin, C. R. *J. Electrochem. Soc.* **2001**, *148*, A1247−A1253.
(7) Sides, C. R.; Martin, C. R. *Adv. Mater.* **2005**, *17*, 125−128.
(8) Taberna, P. L.; Mitra, S.; Poizot, P.; Simon, P.; Tarascon, J. M. *Nat. Mater.* **2006**, *5*, 567−573.
(9) Arico, A. S.; Bruce, P.; Scrosati, B.; Tarascon, J.-M.; van Schalkwijk, W. *Nat. Mater.* **2005**, *4*, 366−377.
(10) Chan, C. K.; Peng, H.; Twesten, R. D.; Jarausch, K.; Zhang, X. F.; Cui, Y. *Nano Lett.* **2007**, *7*, 490−495.
(11) Poizot, P.; Laruelle, S.; Grugeon, S.; Dupont, L.; Tarascon, J. M. *Nature* **2000**, *407*, 496−9.
(12) Yang, R.; Wang, Z.; Liu, J.; Chen, L. *Electrochem. Solid-State Lett.* **2004**, *7*, A496−A499.
(13) Fu, Z.-W.; Wang, Y.; Zhang, Y.; Qin, Q.-Z. *Solid State Ionics* **2004**, *170*, 105−109.
(14) Kang, Y.-M.; Song, M.-S.; Kim, J.-H.; Kim, H.-S.; Park, M.-S.; Lee, J.-Y.; Liu, H. K.; Dou, S. X. *Electrochim. Acta* **2005**, *50*, 3667−3673.
(15) Nam, K. T.; Kim, D.-W.; Yoo, P. J.; Chiang, C.-Y.; Meethong, N.; Hammond, P. T.; Chiang, Y.-M.; Belcher, A. M. *Science* **2006**, *312*, 885−888.
(16) Needham, S. A.; Wang, G. X.; Konstantinov, K.; Tournayre, Y.; Lao, Z.; Liu, H. K. *Electrochem. Solid-State Lett.* **2006**, *9*, A315−A319.
(17) Binotto, G.; Larcher, D.; Prakash, A. S.; Urbina, R. H.; Hegde, M. S.; Tarascon, J. M. *Chem. Mater.* **2007**, *19*, 3032−3040.
(18) Shaju, K. M.; Jiao, F.; Debart, A.; Bruce, P. G. *Phys. Chem. Chem. Phys.* **2007**, *9*, 1837−1842.
(19) Li, Y.; Tan, B.; Wu, Y. *J. Am. Chem. Soc.* **2006**, *128*, 14258−14259.
(20) Iwakura, C.; Fukumoto, Y.; Inoue, H.; Ohashi, S.; Kobayashi, S.; Tada, H.; Abe, M. *J. Power Sources* **1997**, *68*, 301−303.
(21) Laruelle, S.; Grugeon, S.; Poizot, P.; Dolle, M.; Dupont, L.; Tarascon, J. M. *J. Electrochem. Soc.* **2002**, *149*, A627−A634.
(22) Obrovac, M. N.; Dunlap, R. A.; Sanderson, R. J.; Dahn, J. R. *J. Electrochem. Soc.* **2001**, *148*, A576−A588.

(23) Ishihara, T.; Kawahara, A.; Nishiguchi, H.; Yoshio, M.; Takita, Y. *J. Power Sources* **2001**, *97*−*98*, 129−132.
(24) Armstrong, A. R.; Armstrong, G.; Canales, J.; Garcia, R.; Bruce, P. G. *Adv. Mater.* **2005**, *17*, 862−865.
(25) Park, M.-S.; Wang, G.-X.; Kang, Y.-M.; Wexler, D.; Dou, S.-X.; Liu, H.-K. *Angew. Chem., Int. Ed.* **2007**, *46* (750−753), S750/1−S750/4.
(26) Li, W.-Y.; Xu, L.-N.; Chen, J. *Adv. Funct. Mater.* **2005**, *15*, 851−857.
(27) Gao, X. P.; Bao, J. L.; Pan, G. L.; Zhu, H. Y.; Huang, P. X.; Wu, F.; Song, D. Y. *J. Phys. Chem. B* **2004**, *108*, 5547−5551.
(28) Chen, J.; Xu, L.; Li, W.; Gou, X. *Adv. Mater.* **2005**, *17*, 582−586.
(29) Li, W.; Cheng, F.; Tao, Z.; Chen, J. *J. Phys. Chem. B* **2006**, *110*, 119−124.
(30) Wang, Y.; Fu, Z.-W.; Qin, Q.-Z. *Thin Solid Films* **2003**, *441*, 19−24.
(31) Kang, Y.-M.; Kim, K.-T.; Kim, J.-H.; Kim, H.-S.; Lee, P. S.; Lee, J.-Y.; Liu, H. K.; Dou, S. X. *J. Power Sources* **2004**, *133*, 252−259.
(32) Morales, J.; Sanchez, L.; Martin, F.; Ramos-Barrado, J. R.; Sanchez, M. *Electrochim. Acta* **2004**, *49*, 4589−4597.

NL0725906